13th Australasian Fluid Mechanics Conference
Monash University, Melbourne, Australia
13-18 December 1998

PREDICTION OF A PLANE MIXING LAYER USING VARIOUS LINEAR AND NON-LINEAR K-ε MODELS

J. A. Naser

School of Engineering & Science, Swinburne University, Hawthorn, Victoria 3122, AUSTRALIA

ABSTRACT

The paper evaluates performances of four linear and non-linear variants of k-ε model in predicting a 2-D plane mixing layer. The variants include: (i) standard k-ε model; (ii) k-ε model, where production of ε is augmented by the irrotational strains; (iii) k- ε - γ model, where the eddy viscosity is modified with a function of intermittency factor ; (iv) non-linear k- ε model, extended to account for turbulence anisotropy. The governing equations are discretised using a finite volume technique. The central Differencing scheme was employed to evaluate the diffusion terms and Linear upwind differencing scheme was employed to evaluate the convection terms. The solutions were obtained using the PISO (Pressure Implicit with Splitting of Operator) algorithm. The results obtained with the modified versions show much improved agreement as compared with the standard k- ε . However the models failed to reproduce the full qualitative and quantitative features.

INTRODUCTION

The development of plane mixing layer is controlled by the transverse two dimensional vortical structure with cross-sectional dimensions of the same order as the shear-layer thickness (Brown & Roshko (1974)). Winant & Brownand (1974) showed that the interaction of these transverse vortices ultimately results in a vortex paring process, which controls the production of the Reynolds-stress and the growth of the mixing layer. Inspite of the complexity of the flow, the simple concepts of eddy viscosity and eddy diffusivity appear to be valid within the turbulent mixing layer (Wygnaski & Fiedler (1970)). However, the most widely used eddy viscosity turbulence model, the standard k-ε model, fails to reproduce the mean velocities observed in the experiments. Rodi et al. (1980) showed that the difference between the k-ε predictions and the measurements manifest themselves mainly to the over prediction of shear stresses. Hanjalic & Launder (1980) argued that this over prediction may be reduced by increasing the production of energy dissipation rate. Cho & Chung (1992) applied k- ε - γ model and obtained improved results. This is because the intermittency factor γ takes care of the outer layer contaminated by the irrotational flow. The structure of turbulence inside the mixing layer is non-homogenous and anisotropic. The non-linear k-ε model (Speziale (1987)) is expected to take account of anisotropic turbulence. The objective of the present work is to predict the development of a plane mixing layer using linear and non-linear versions of k-ε model and evaluate their performances.

SOLUTION DOMAIN & BUNDARY CONDITIONS

The two dimensional plane mixing layer investigated here is shown in Fig.1. This study is a numerical simulation of a part of the experimental investigation carried out by Yang & Karlsson (1991). Inlet velocity profiles were obtained from experimental values of displacement and momentum thickness. Inlet turbulent kinetic energy is taken as 0.03% of inlet mean kinetic energy (as per experimental data). Inlet turbulence length scale according to Escudier(1966):

$$l_\varepsilon = C_\mu^{\frac{1}{4}} \kappa y \quad \text{if } \kappa y \le (0.09\delta) \text{ ; and}$$

$$l_\varepsilon = C_\mu^{\frac{1}{4}} (0.09\delta) \quad \text{if } \kappa y > (0.09\delta);$$

where δ is the boundary layer thickness. Inlet intermittency, γ, is obtained from the distribution of γ in a flat plate boundary layer.

THE GOVERNING EQUATIONS

For turbulent, incompressible flow of a Newtonian fluid, the time averaged governing equations, take the form:

continuity
$$\frac{\partial u_i}{\partial x_i} = 0 \qquad (1)$$

momentum
$$\frac{\partial u_i}{\partial t} + \frac{\partial\left(u_i u_j\right)}{\partial x_j} = -\frac{1}{\rho}\frac{\partial p}{\partial x_i} + \frac{1}{\rho}\frac{\partial}{\partial x_j}\left[\mu_l\left(\frac{\partial u_i}{\partial x_j} + \frac{\partial u_j}{\partial x_i}\right) - \rho\overline{u'_i u'_j}\right] \qquad (2)$$

When closure is achieved through the linear k-ε model, the Reynolds stress tensor is modelled as:

$$-\rho\overline{u'_i u'_j} = \mu_t\left(\frac{\partial u_i}{\partial x_j} + \frac{\partial u_j}{\partial x_i}\right) \qquad (3)$$

Where the turbulent viscosity μ_t is obtained as $\mu_t = \frac{\rho c_\mu k^2}{\varepsilon}$. The turbulence kinetic energy (k) and its dissipation rate (ε) are obtained from their equations given as:

k-equation
$$\frac{\partial k}{\partial t} + \frac{\partial(u_j k)}{\partial x_j} = \frac{1}{\rho}\frac{\partial}{\partial x_j}\left[\frac{\mu}{\sigma_k}\left(\frac{\partial k}{\partial x_j}\right)\right] + G - \varepsilon \qquad (4)$$

ε–equation

$$\frac{\partial \varepsilon}{\partial t}+\frac{\partial (u_j \varepsilon)}{\partial x_j}=\frac{1}{\rho}\frac{\partial}{\partial x_j}\left[\frac{\mu}{\sigma_\varepsilon}\left(\frac{\partial \varepsilon}{\partial x_j}\right)\right]+C_1\frac{\varepsilon}{k}-C_2\frac{\varepsilon^2}{k} \qquad (5)$$

Here μ is the effective viscosity given by:

$$\mu=\mu_l+\mu_t \qquad (6)$$

and G is the generation term, which, according to the standard k-ε (Launder & Spalding (1974)) is given by:

$$G=\mu_t\frac{\partial u_i}{\partial x_j}\left(\frac{\partial u_i}{\partial x_j}+\frac{\partial u_j}{\partial x_i}\right) \qquad (7)$$

The values of the empirical constants used in the standard k-ε are given below:

$C_\mu=0.09,\ C_1=1.44,\ C_2=1.92,\ \sigma_k=1.0,\ \sigma_\varepsilon=1.3$

(Launder & Spalding (1974))

In the present study, the following four turbulence models are chosen in the light of the discussion presented in the last sub-section.

1. The standard k-ε, here after called the KE.

2. A modification of the k-ε , in which the generation of ε is preferentially promoted by the irrotational strains, by replacing the production of ε ($p_\varepsilon \equiv C_1\frac{\varepsilon}{k}G$) in equation (5) by the following term:

$$p_\varepsilon=\frac{\varepsilon}{k}\left\{\begin{matrix}C_{\varepsilon 1}\mu_t\left(\frac{\partial u_i}{\partial x_j}+\frac{\partial u_j}{\partial x_i}\right)(1-\delta_{ij})\\ +C_{\varepsilon 2}\mu_t\left(\frac{\partial u_i}{\partial x_j}+\frac{\partial u_j}{\partial x_i}\right)\delta_{ij}\end{matrix}\right\}\left(\frac{\partial u_i}{\partial x_j}\right) \qquad (8)$$

where $C_{\varepsilon 1}$ =1.44 and $C_{\varepsilon 2}$ =14.65; δ_{ij} =1 if i=j and δ_{ij} =0 if i ≠ j. This modification was made following the recommendation from Hanjalic & Launder (1980). Where they argued that, energy transfer rates across the turbulence spectrum are preferentially promoted by irrotational deformations and since energy in transit across the spectrum ends up as energy dissipated, rates of energy dissipation for irrotational strains must be higher than that for rotational strains. They recommended a value of $C_{\varepsilon 2}$ =4.44, whereas in the present study a three times higher value had to be used in order to obtain closer agreement with the experiments. This model will hereafter be called the KEM model.

3. k-ε model, modified with an intermittency factor γ. In this model, in addition to the transport equations for k (Eq.4) and ε (Eq. 5), the following transport equation for the intermittency factor γ, is solved:

γ–equation

$$\frac{\partial \gamma}{\partial t}+\frac{\partial (u_j \gamma)}{\partial x_j}=\frac{1}{\rho}\frac{\partial}{\partial x_j}\left[(1-\gamma)\frac{\mu_t}{\sigma_g}\left(\frac{\partial \gamma}{\partial x_j}\right)\right]+C_{g1}\gamma(1-\gamma)\frac{G}{k}+C_{g2}\frac{k^2}{\varepsilon}\frac{\partial \gamma}{\partial x_j}\frac{\partial \gamma}{\partial x_j}-C_{g3}\gamma(1-\gamma)\frac{\varepsilon}{k}\Gamma \qquad (9)$$

Where

$$\Gamma \equiv \frac{k^{(5/2)}}{\varepsilon^2}\frac{u_i}{\left(u_k u_k\right)^{1/2}}\frac{\partial u_i}{\partial x_j}\frac{\partial \gamma}{\partial x_j} \qquad (10)$$

The eddy-viscosity μ_t is then obtained by a function:

$$\mu_t=\frac{C_\mu}{\rho}\left[\frac{1+C_{\mu g}\frac{k^3}{\varepsilon^2}\gamma^{-3}}{(1-\gamma)\frac{\partial \gamma}{\partial x_k}\frac{\partial \gamma}{\partial x_k}}\right]\frac{k^2}{\varepsilon} \qquad (11)$$

This model, hereafter called the k-ε–γ, is taken from Cho & Chung (1992). This class of model, incorporating intermittency, is developed on the basis of the observation that, a turbulence model constructed essentially for fully turbulent flows can not be expected to work in the outer layer contaminated with the irrotational flow. The values of the empirical constants used in the KEG model are :

$C_{g1}=1.6,\quad C_{g2}=0.15,\quad C_{g3}=0.16,$

$C_{\mu g}=0.1,\quad \sigma_g=1.0$ (Cho & Chung (1992))

4. A non-linear k-ε model. In this model, the transport equations for k (Eq. 4) and ε (Eq. 5), are solved and the Reynolds stress is obtained as:

$$-\rho\overline{u_i' u_j'}=\rho C_\mu\frac{k^2}{\varepsilon}\overline{D_{ij}}+\rho C_D\left(C_\mu\frac{k^{3/2}}{\varepsilon}\right)^2\left(\overline{D_{im}}\,\overline{D_{mj}}-\frac{1}{3}\overline{D_{mn}}\,\overline{D_{mn}}\,\delta_{ij}\right)+\rho C_E\left(C_\mu\frac{k^{3/2}}{\varepsilon}\right)^2\left(\overline{\overline{D_{ij}}}-\frac{1}{3}\overline{\overline{D_{mn}}}\,\delta_{ij}\right) \qquad (12)$$

where $$\overline{D_{ij}}=\frac{1}{2}\left(\frac{\partial u_i}{\partial x_j}+\frac{\partial u_j}{\partial x_i}\right) \qquad (13)$$

and

$$\overline{\overline{D_{ij}}} = \frac{\partial \overline{D_{ij}}}{\partial t} + u_k \frac{\partial \overline{D_{ij}}}{\partial x_k} - \frac{\partial u_i}{\partial x_k}\overline{D_{kj}} - \frac{\partial u_j}{\partial x_k}\overline{D_{ki}} \qquad (14)$$

The values of the constants are:

$C_D = C_E = 1.68$ Speziale (1987)

Due to the formation and the mutual interaction of transverse vortices, the structure of turbulence inside the mixing layer is non-homogenous and anisotropic. Therefore, the assumptions leading to the formulation of the k-ε model are inadequate for plane mixing layer flow. To extend the validity of the k-ε to this type of flow Speziale (1987) developed this model. This model will hereafter be called as the NLKE model.

THE SOLUTION PROCEDURE

The governing equations are discretised in a finite volume fashion using a staggered arrangement of variables. The Central Difference Scheme (CDS) was employed to evaluate the diffusion terms and Linear Upwind Scheme (LUDS) was employed to evaluate the convection terms. The solutions were obtained using the PISO (Pressure-Implicit with Splitting of Operators) algorithm of Issa (1984). 300 grids in the stream-wise direction and 100 grids in the cross-stream direction were found to give grid independent results.

RESULTS AND DISCUSSIONS

The velocity profiles are presented in Figs. 2-4. Here $\lambda = u_{av}/f_n$; u_{av} is the average velocity and f_n is the natural frequency of instability of mixing layer (Yang & Karlsson (1991)). At x/λ =1.875 (Fig.2) the results obtained with KEG are in good agreement with the experiments, specially the wake like region is very well reproduced. The NLKE and the KEM models under predict this wake effect and KE is almost insensitive to it. At x/λ =8.125 (Fig.3), measurements show that the wake has disappeared and the mixing layer is spreading out. But the KEG results still continue to show this wake effect. NLKE and KEM results are in improved agreement with the measurements but KE results again show worst comparisons associated with the over prediction of the shear layer thickness. Further downstream At x/λ =15.625 (Fig.4) the KE results continues to show over prediction of the shear layer thickness whereas KEG and NLKE models show under prediction. The KEM model results show minor under prediction on the accelerating region, but the agreement on the decelerating side is reasonably good.

At x/λ =1.875, although the KEG model shows high turbulence intensity (Fig.5) and higher length scale (Fig. 8), the eddy viscosity calculated from Eq. (11) assumes relatively lower values in the core region of the shear layer. This is due to inclusion of the gradient of intermittency term in Eq. (11), which has the minimum value in the centre of the shear layer core. These lower eddy viscosity values ultimately leads to lower shear stresses, which made it possible to reproduce the wake like region at x/λ =1.875 (Fig.2). Due similar reasons KEG continues to predict lower shear stresses at the downstream locations, x/λ =8.125 & 15.625, leading to lower shear layer thicknesses. Unfortunately these shear layer thicknesses are lower than that observed in the experiments. The values of turbulence intensities and length scales obtained with KEM are much lower than that obtained with the other models (Figs.5-10). This is due to higher production of ε from irrotational strains. The mean velocity profiles suggests that, this higher production of ε: is not sufficient enough to reproduce the wake effect at x/λ =1.875 and is exaggerated at x/λ =15.625 leading to the under prediction of the shear layer. The NLKE results show that the inclusion of non-linear effects has produced the minimum values of turbulence intensities and length scales in almost all the locations. But these lower values seems to be relatively high at x/λ =1.875 leading to the failure to reproduce the wake effect and relatively low at x/λ =15.625 leading to the under prediction of the shear layer.

It is clear from the results presented above that, in predicting developing shear layer, improved agreement can be obtained with KEG, KEM and NLKE. These improvements are realised through elimination and/or reduction of the tendency of the KE to give higher shear stress values. However the models failed to reproduce the full qualitative and quantitative features of the flow.

CONCLUSIONS

The paper has concentrated on the performance of four variants of k-ε model in predicting a 2-D plane mixing layer. Ad-hoc modification of the k-ε models can apparently improve the agreement between the prediction and the experiment. But the true physics of the flow is not reproduced. These improvements are realised through elimination and/or reduction of the tendency of the k-ε model to give higher shear stress values. The improvements are not consistent in all the regions of the flow domain. Hence the modifications does not have general superiority.

REFERENCES

BROWN, G.L., and ROSHKO, A., 1974, "On density effects and large structures in turbulent mixing layers", *J.Fluid Mech.*, Vol., 64, pp. 775-816

CHUNG, M.K., and CHO, J.R., 1992, "K-ε-γ equation turbulence model", *J.Fluid Mech.*, Vol. 237, pp. 301

ESCUDIER, M.P., 1966, "The distribution of mixing length in turbulent flow near walls", *Imperial College Heat Transfer Report* TWF/Tn11

HANJALIC, K., and LAUNDER, B.E., 1990, "Sensitising the dissipation equation to irrotational strains", *J. Fluid Engineering*, Vol. 102.

ISSA, R.I., 1984, "Solution of the Implicitly Discretised Fluid Flow Equations by Operator Splitting", *J. Comp. Physics*, Vol. 62, No.1

LAUNDER, B. E., and SPALDING, D. B., 1974, "The numerical computation of turbulent flow", *Comp. Methods Appl. Mech. Engng*. Vol. 3, pp. 269

RODI, W., CELIK, I., DEMUREN, A. O., SCHEUERER, G., SHIRANI, I., LESCHZINER, M.A., and RASGOYI, A.K., *proc. of 1980-1, AFOSR-HTTM-Stanford conf. on complex turbulent flows*, Vol.III p1495

SPEZIALE, C. G., 1987, "On nonlinear k-l and k- ε models of turbulence", *J. Fluid Mech.*, Vol. 178, p459

WINANT, C. D., and BROWAND, F.K., 1974, "Vortex paring: The mechanism of turbulent mixing layer growth at moderate Reynolds number", *J. Fluid Mech.*, Vol. 63, pp. 237-255

WYGNANSKI, I, and FIEDLER, H.E., 1970, "The two dimensional mixing region", *J. Fluid Mech.*, Vol. 41, part 2, pp.327-361

YANG, Z., and KARLSSON, S.K.F., 1991, "Evolution of Coherent structures in plane shear layer", *Phys. Of Fluids* A, Vol.3, No.9.

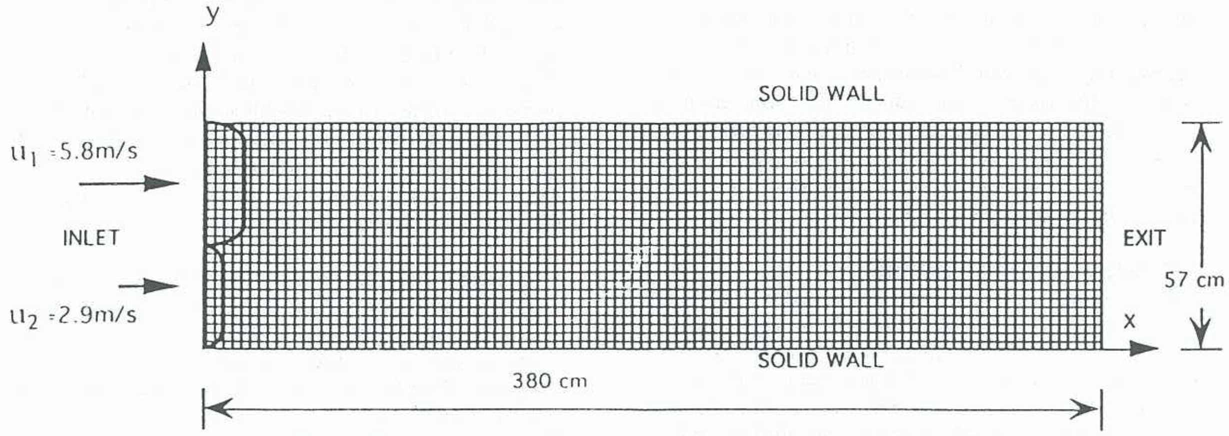

Fig. 1 Solution domain (grids shown are representative only)

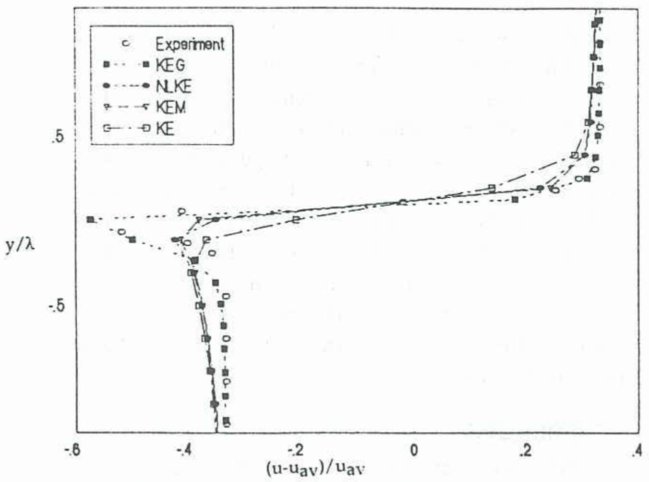

Fig. 2 Streamwise velocity profile at x/λ=1.875.

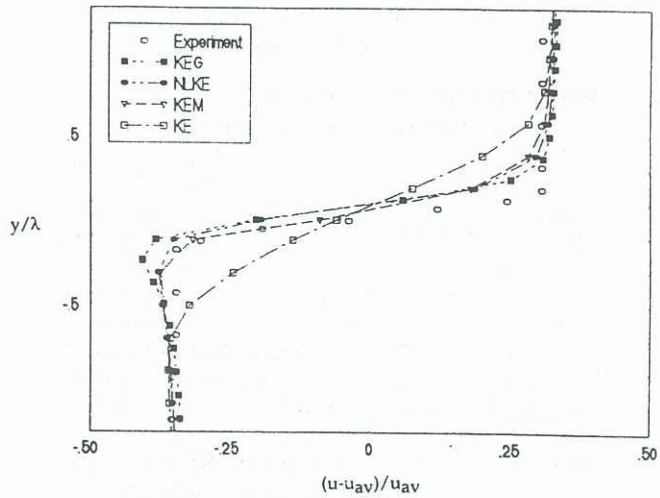

Fig. 3 Streamwise velocity profile at x/λ=8.125.

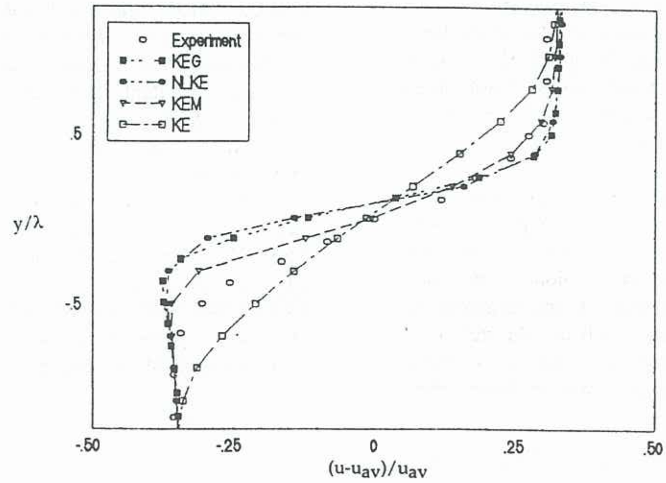

Fig. 4 Streamwise velocity profile at x/λ=15.625.

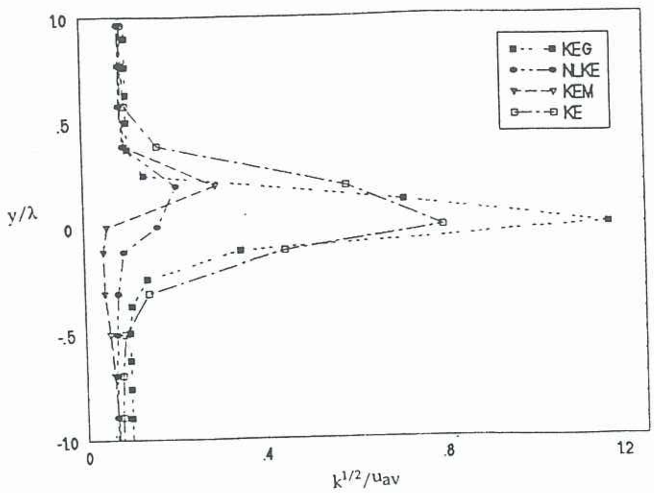

Fig. 5 Cross-stream turbulence intensity profile at $x/\lambda=1.875$.

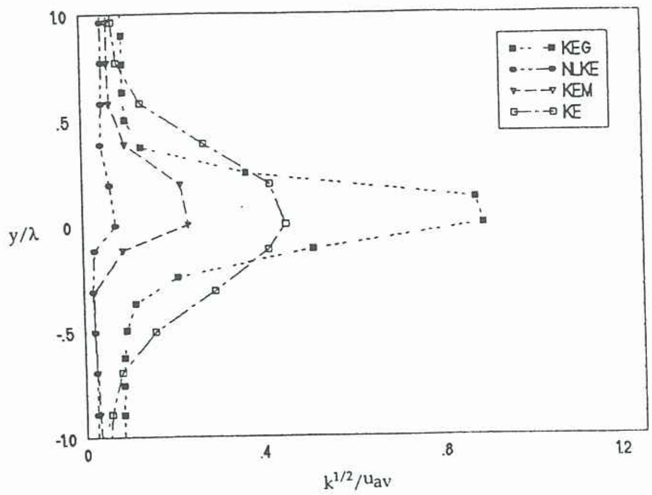

Fig. 6 Cross-stream turbulence intensity profile at $x/\lambda=8.125$.

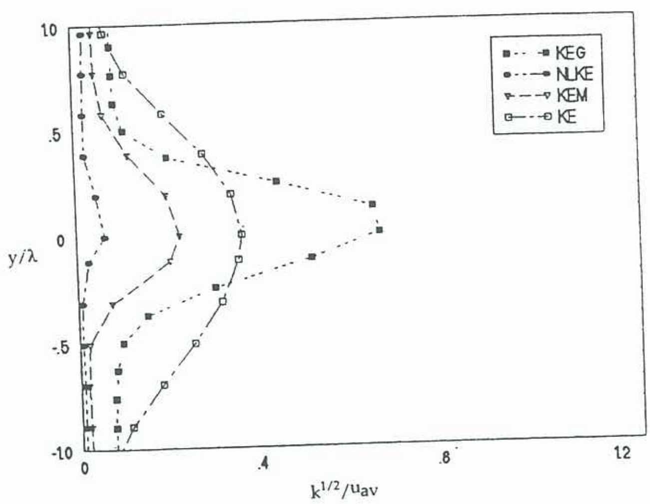

Fig. 7 Cross-stream turbulence intensity profile at $x/\lambda=15.625$

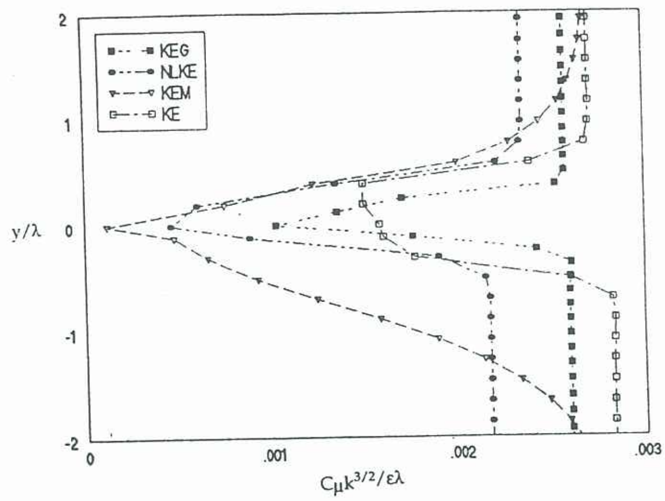

Fig. 8 Cross-stream turbulence length-scale profile at $x/\lambda=1.875$

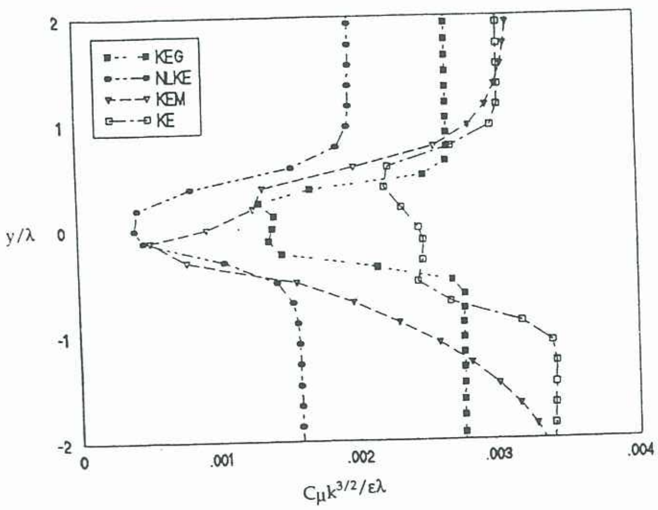

Fig. 9 Cross-stream turbulence length-scale profile at $x/\lambda=8.125$.

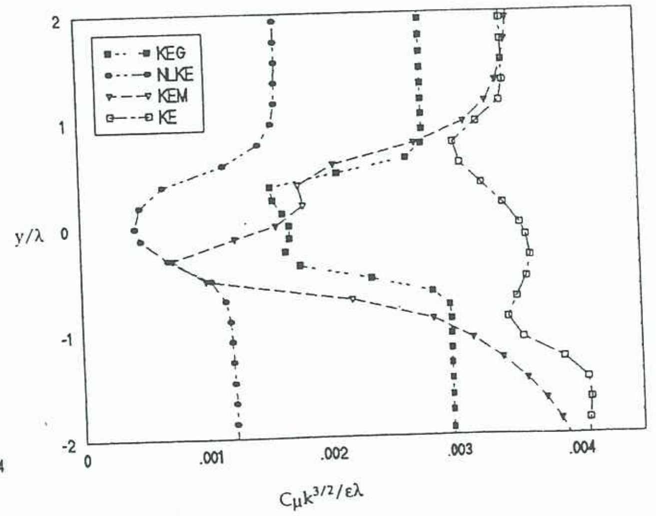

Fig. 10 Cross-stream turbulence length-scale profile at $x/\lambda=15.625$